

The Glueckstadt Graben of the North-German Basin: new insights into the structure from 3D and 2D gravity analyses

Tamara Yegorova · Yuriy Maystrenko ·
Ulf Bayer · Magdalena Scheck-Wenderoth

Received: 3 May 2007 / Accepted: 6 July 2007 / Published online: 28 July 2007
© Springer-Verlag 2007

Abstract The structure of the Glueckstadt Graben has been investigated by use of 3D gravity backstripping technique and by 2D gravity and magnetic modelling. Subtracting the gravity effects of the Meso-Cenozoic sediments together with Permian salt reveals a positive residual anomaly within the Glueckstadt Graben. This anomaly includes two local maxima over the Westholstein and Eastholstein Troughs. The 2D gravity models point to the presence of a high-density body within the lower crust of the Glueckstadt Graben. In addition, the results of 2D magnetic modelling indicate that the central part of the high-density body is overlain by an area with high susceptibility. Most probable, the formation of this high-density body is a result of complex poly-phase tectonic history of the study area. Finally, the results of gravity modelling indicate that Permian salt is not homogeneous. 3D gravity analysis and, especially, 2D gravity modelling have distinguished the differences in degree of salt saturation in salt-rich bodies, and elucidate the proportion of Rotliegend salt.

Keywords Glueckstadt Graben · 3D and 2D gravity analyses · 2D magnetic modelling · Permian salt

Introduction

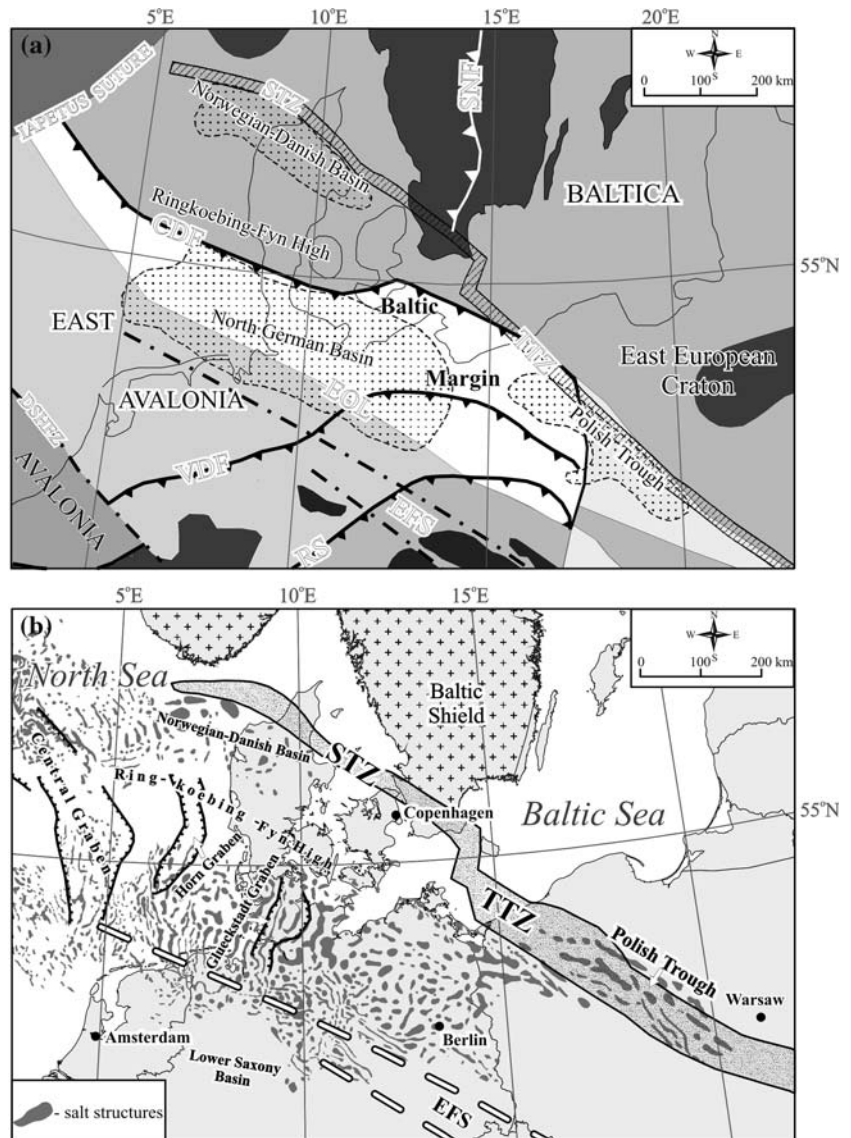
The Central European Basin System and its sub-basins, the Norwegian-Danish Basin, the North German Basin, and the Polish Trough developed over a heterogeneous crust along the transition between the Precambrian East European Craton/Baltic Shield and the relative young Phanerozoic crust below the rest of the basin system (Fig. 1a). During the last two decades, results of gravity analysis have produced insights into basin and crustal structure of the Central European Basin System (Hermes 1986; Dohr et al. 1989; Brink et al. 1994; Scheck and Bayer 1999; Bachmann and Grosse 1989; Zhou and Thybo 1996, 1997; Krolkowski and Grobelny 1991; Dirkzwager et al. 2000; Olesen et al. 2004; Lyngsie et al. 2006; Yegorova et al. 2007). One of the major problems of gravity modelling within the Central European Basin System is related to gravity effects resulting from large salt structures (see Fig. 1b), which formed during the Meso-Cenozoic due to activation of Permian salt. This is one of the first-order problems in gravity modelling because the huge salt structures provide a density deficit creating gravity signals in the observed field. Yegorova et al. (2007) tried to estimate the gravity effect of salt structures at the regional scale by assigning the lateral density variations within the sediments. It was shown that the effect of large salt structures can reach 30 mGal in amplitude and can partly explain the Helgoland and the Glueckstadt gravity lows in the western part of the North German Basin (Fig. 2a; Yegorova et al. 2007).

In general, the map of the observed gravity field over the Central European Basin System (Fig. 2a) shows a rather heterogeneous pattern with regard to the various sub-basins. The Polish Trough is characterised by a strong gravity low while the area of the North German Basin and Norwegian-Danish Basin is strongly complicated by short

T. Yegorova · Y. Maystrenko (✉) · U. Bayer ·
M. Scheck-Wenderoth
GeoForschungsZentrum Potsdam,
Telegrafenberg C426, 14473 Potsdam, Germany
e-mail: yuram@gfz-potsdam.de

T. Yegorova
Institute of Geophysics,
National Academy of Sciences of Ukraine,
03680 Kiev, Ukraine

Fig. 1 **a** Structural sketch map of the Central European Basin System; **b** location of the Glueckstadt Graben in relation to other Triassic basins within the Central European Basin System (position of salt structures after Vejbaek and Britze 1994; Lockhorst 1998; Baldschuhn et al. 2001; Evans et al. 2003; Dadlez 2003). Major structural elements after Pharaoh (1999): *CDF* Caledonian Deformation Front, *DSHFZ* Dowsing-South Hewett Fault Zone, *EOL* Elbe-Odra Line, *EFS* Elbe Fault System, *RS* Reic Suture, *SNF* Sveco-Norwegian Front, *STZ* Sorgenfrei-Tornquist Zone, *TTZ* Teyseyre-Tornquist Zone, *VDF* Variscan Deformation Front

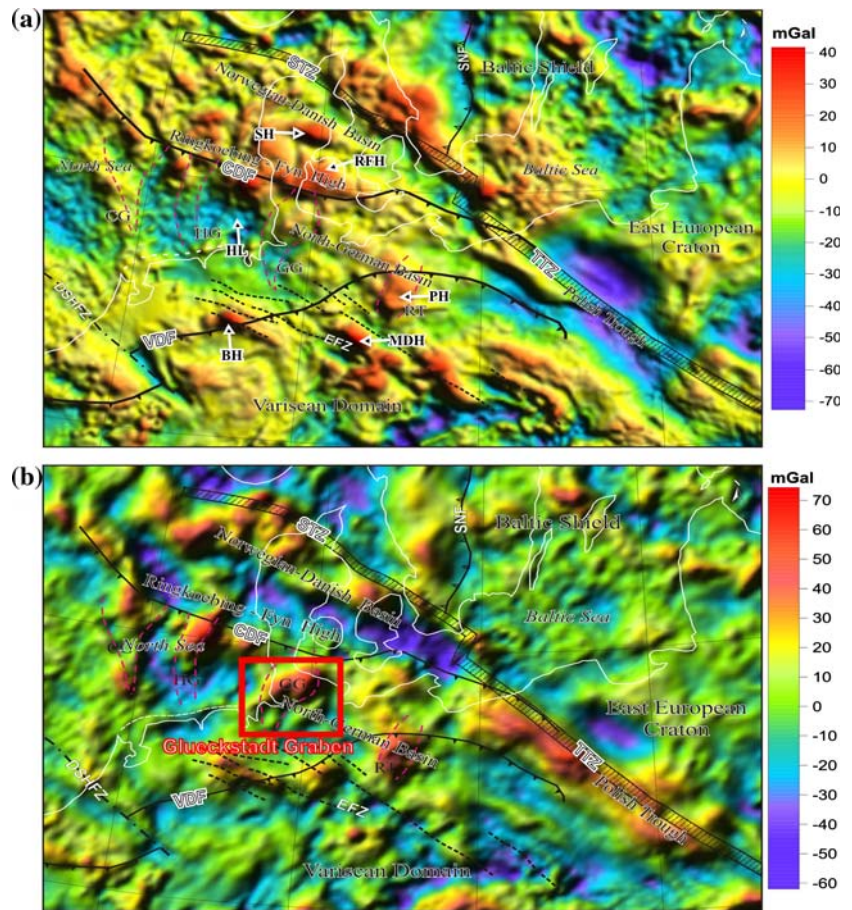


wavelength fluctuations in the Bouguer anomalies (Fig. 2 a). The short wave components (after removing the influence of the sediments, the Moho topography, the large scale crustal heterogeneities and the long-wave component of the residual field) correlate well with Triassic grabens and inversion features (Fig. 2b). This correlation indicates that these structures may be deeply rooted. However, some uncertainties remain concerning the resolution of the model used. To resolve these, an attempt has been made to look inside of the Glueckstadt Graben by use of 3D gravity backstripping, based on a 3D structural model of the deepest Triassic structure of the Central European Basin System, the Glueckstadt Graben (see Fig. 3; Maystrenko et al. 2006). In addition, a detailed density model was performed along two cross-sections across the central part of the Glueckstadt Graben and was supplemented by 2D magnetic modelling.

Regional overview

The area under consideration is a central segment of the Central European Basin System, which is located in northwestern Germany (Fig. 1). Tectonically, the Glueckstadt Graben is situated between two deep reaching fault systems, the Caledonian Deformation Front (CDF) along the southern margin of the Ringkøbing-Fyn High in the north and the Elbe Fault System (EFS) in the south (Fig. 1a). Additionally, the Elbe-Odra Line crosses the southern part of the study area. The results of the passive teleseismic experiment TOR indicate a regional thinning of the lithosphere from the Baltic Shield towards the Glueckstadt Graben with two pronounced steps beneath the Sorgenfrei-Tornquist Zone and the Elbe-Odra Line (Gрегersen et al. 2002; Plomerova et al. 2002; Shomali et al. 2006).

Fig. 2 **a** Map of the observed gravity field of the Central European Basin System. Data from the data base (Wybraniec et al. 1998); **b** short-wave component responsible for small crustal heterogeneities, has been derived by subtracting the influence of the sediments, Moho topography, large-scale crustal heterogeneities and the long-wave component of the residual field (Yegorova et al. 2007). For major structural elements see Fig. 1. Grabens and troughs: *CG* Central Graben, *GG* Glueckstadt Graben, *HG* Horn Graben, *RT* Rheinsberg Trough. Gravity highs and lows: *BH* Bramsche High; Magdeburg-Dessau High; *HL* Helgoland Low; *PH* Pritzwalk High; *RFH* Ringkoebing-Fyn High; *SH* Sylt High



Many geological and geophysical studies have been performed within the Glueckstadt Graben. The detailed structure of the sedimentary cover was intensively studied by commercial drilling and seismic exploration in the context of oil and gas exploration. The results of industrial seismic data interpretation have been published by Trusheim (1960), Sannemann (1968), Dohr et al. (1989), Brink et al. (1990, 1992), Baldschuhn et al. (1996, 2001), Kockel (2002, 2003), Maystrenko et al. (2005a, b) and many others. In general, the Glueckstadt Graben reflects the main tectonic stages of the Central European Basin System with some superposed local features. The Central European Basin System originated during the end of Late Carboniferous-Early Permian times when the study area was affected by extensive igneous activity and faulting (Gast 1988; Plein 1990; Ziegler 1990; Dadlez et al. 1995; Bachmann and Hoffmann 1997; Bayer et al. 1999; Abramovitz and Thybo 1999). At that time, two east-west elongated basins developed in central Europe, named the Northern and Southern Permian basins. Significant amount of salt accumulated during the Late Permian in these two basins. The reconstruction of the initial Permian salt thickness (Maystrenko et al. 2005b) indicates that the Glueckstadt Graben was a centre of subsidence at the end

of the Permian. During post-Permian times, the initially thick Permian salt (salt-rich Rotliegend plus Zechstein) complicated the subsidence pattern of the study area due to its withdrawal from the source layer into huge salt walls, diapirs and pillows (see Fig. 3). During the Triassic, Jurassic and Early Cretaceous, the Central European Basin System was affected by several pulses of extensional tectonics which led to the formation of the superimposed sub-basins, such as the Scagerrak and Brande Grabens, the Glueckstadt Graben and Rheinsberg Trough, the Lower Saxony Basin and the North Sea basins (Sole Pit Basin, Central and Horn Grabens). The main subsidence stage of the Glueckstadt Graben occurred during the Triassic extension with culmination in the Late Triassic (Keuper) when up to 6,000 m of sediments were deposited, forming its central part (Fig. 3a). During the Jurassic, three SW-NE-aligned marginal troughs (Eastholstein, Westholstein and Hamburg; see Fig. 3a) developed in relation to the Central Glueckstadt Graben under predominance of an extensional regime within the area. There is a major Late Jurassic-Early Cretaceous unconformity within the study area. The cause of the Late Jurassic-Early Cretaceous interruption of sedimentation is still not clear and can be related to a regional sea level fall or relative uplift of the

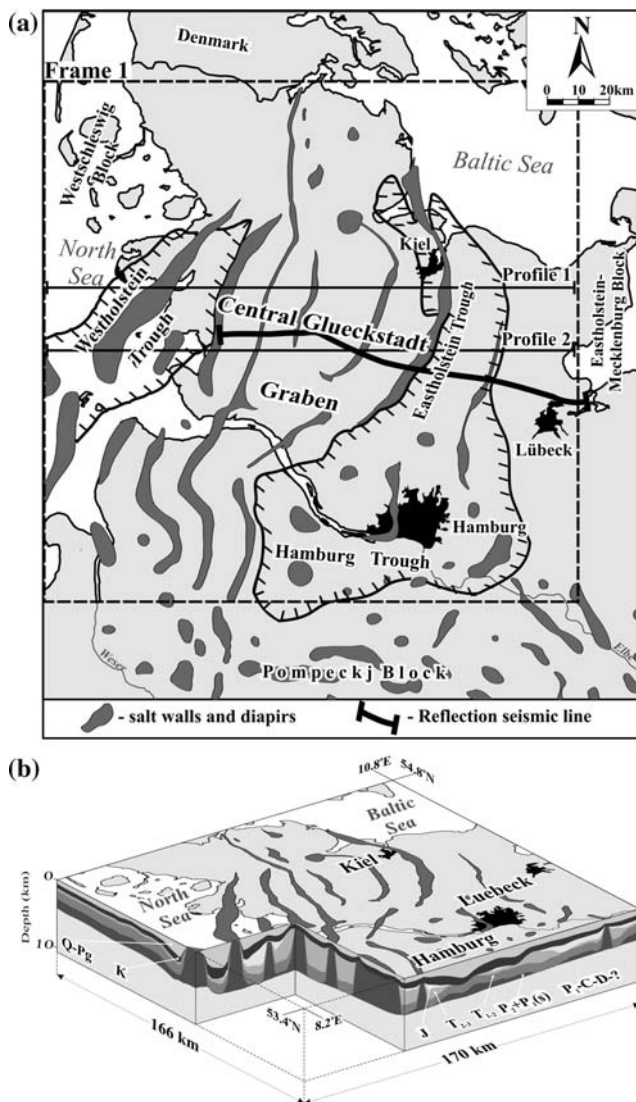


Fig. 3 **a** Tectonic map of the Glueckstadt Graben with location of the seismic line and modeled profiles (position of salt domes by Baldschuhn et al. 2001). **b** 3D structural model of the Glueckstadt Graben and adjacent areas (Maystrenko et al. 2006). Stratigraphic key: *P₁-C-D* Undivided Lower Permian (Rotliegend), Carboniferous and Devonian deposits; *P₂ + P_{1(s)}* upper part of the Lower Permian and Upper Permian (undivided Zechstein and salt-rich Rotliegend); *T* Triassic; *J* Jurassic; *K* Cretaceous; *Pg* Paleogene; *Q-N* Quaternary-Neogene

area. In the Late Cretaceous, the Alpine orogeny caused compressional stresses within the entire Central European Basin System with strain localization along the EFS, the Teisseyre-Tornquist Zone and the Sorgenfrei-Tornquist Zone (Ziegler 1990; Scheck et al. 2002; Otto 2003; Scheck-Wenderoth and Lamarche 2005; Mazur et al. 2005; Krzywiac 2006). The Glueckstadt Graben was not essentially inverted during the Late Cretaceous-Early Tertiary when reverse faults and flexures developed along the EFS in the south. In the Glueckstadt Graben, the Late Creta-

ceous-Early Tertiary compression caused increased salt activity (Kockel 2002; Maystrenko et al. 2006). In the Cenozoic, a depocentre developed within the central North Sea (Ziegler 1990; Scheck-Wenderoth and Lamarche 2005). At that time, the study area is characterised by rapid subsidence in the Eastholstein, Westholstein and Hamburg Troughs.

On the other hand, our knowledge about the deep structure and pre-Permian evolution of the Glueckstadt Graben is obscured due to a lack of the deep seismic reflection profiling. Bayer et al. (2002) proposed a Caledonian age of consolidation of the lower crust beneath the Glueckstadt Graben. According to their interpretation, the lower crust of the area under consideration represents the margin of Baltica, which was overthrust during the Caledonian orogeny (Thybo 2001; Bayer et al. 2002). The present-day structure of the lower crust is known from profile 1 of the EUGENO-S of the European Geotraverse (EUGENO-S Working Group 1988; Blundell et al. 1992). However, the reliable velocity model was not derived for the Glueckstadt Graben because it is crossed by the southernmost part of the profile. Consequently, the velocity interfaces were only shown by dashed lines (EUGENO-S Working Group 1988; Blundell et al. 1992). Accordingly, the crust is represented in a rather schematic way with increased velocities with depth from 6,400–6,500 to 6,700 m/s; and the Moho boundary is shown at the depth of 28–30 km (Blundell et al. 1992). Concerning the Moho topography, similar results were achieved from deep industrial seismic lines, which have a record length up to 13 s of TWT (Bachmann and Grosse 1989; Dohr et al. 1989; Brink et al. 1990). On the other hand, recent reprocessing of the key seismic line (for location, see Fig. 3a) implies a smoothed Moho topography beneath the Glueckstadt Graben (Yoon et al. 2005). Therefore, the topography of the Moho is still not clear beneath the study area. Some information about the composition and structure of the crust can be obtained from gravity modelling, showing a vast gravity anomaly beneath the Glueckstadt Graben after the observed gravity field is reduced to the base of the Zechstein (Dohr et al. 1989; Brink et al. 1994). One of possible reasons for this gravity maximum can be related to high-density crust beneath the area under consideration. A similar explanation has been given by Scheibe et al. (2005), who modeled a high-density body (around 3,000 kg/m³) in the crystalline basement extending from the Rheinsberg Trough to the Glueckstadt Graben. Additionally, Scheibe et al. (2005) performed magnetic modelling for the entire North German Basin, which indicates low magnetisation and susceptibility of crystalline basement within the central part of the Glueckstadt Graben with pronounced increasing towards the north and east.

Potential fields

The maps of the initial gravity (Bouguer anomalies onshore and free-air anomalies offshore) and magnetic fields (Fig. 4) were constructed with horizontal resolution of 2 km using the compilation by Trans-European Suture Zone Potential Field Group (Wybraniec et al. 1998).

Gravity data

The gravity map (Fig. 4a) shows the Bouguer anomaly onshore (calculated with density $2,670 \text{ kg/m}^3$) and the free-

air anomaly offshore. At the regional scale, the study area is characterised by the gravity high of Schleswig-Holstein and the gravity low of Glueckstadt within the central and southwestern part of the Glueckstadt Graben (Fig. 2a). The surrounding gravity field is characterised by two pronounced positive anomalies in the north, named the Sylt and the Ringkoebing-Fyn gravity highs (correspondingly the SH and the RFH in Figs. 2a, 4a). In the southwest, the Bramsche anomaly and the gravity high of Magdeburg-Dessau are displayed along the EFS (Fig. 2a). The broad Helgoland Low (HL) over the southeastern North Sea is adjacent to the Glueckstadt Graben in the west. Another spectacular anomaly of the North German Basin, the Pritzwalk (Rheinsberg) High, is located within the central part of the North East German Basin (Fig. 2a).

At the basin scale, the most pronounced feature is the Glueckstadt Low (GL), which reaches up to -26 mGal (Fig. 4a). The almost circular Husum negative anomaly (about -30 mGal) within the broad HL can be seen in the northwestern part of the map. Additionally, two low-amplitude negative anomalies are distinguished within the southeast of the map in Fig. 4a, where the Moelln Low (ML) and the gravity low of Hamburg (HAL) reach amplitudes up to -12 mGal . The highest values of the gravity field (14 mGal) over the Glueckstadt Graben are observed within the Heide anomaly (HH), which has a strong gravity gradient towards the south and southwest (Fig. 4a). The Norderstedt-Kiel (NKH) and Hamburg gravity (HAH) highs are characterised by smaller gravity highs compared with the Heide gravity high, reaching 8 and 2 mGal , respectively.

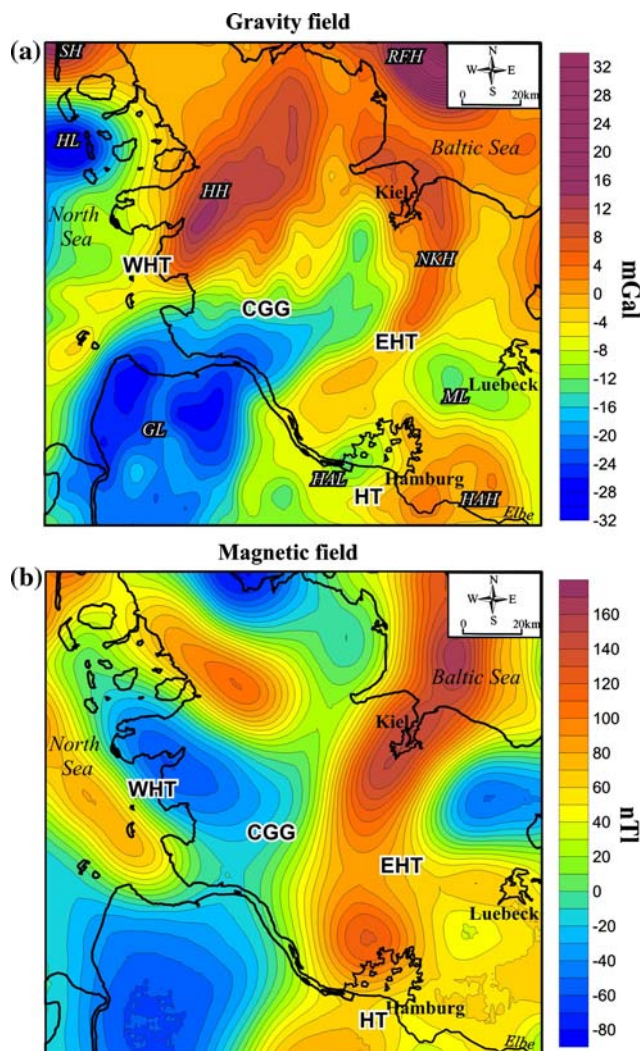


Fig. 4 Maps of the Bouguer gravity anomalies onshore and Free-Air anomalies offshore (a) and aeromagnetic anomalies measured at a height of 700 m (b) over the Glueckstadt Graben. Structural elements: *CTG* Central Glueckstadt Graben, *EHT* Eastholstein Trough, *HT* Hamburg Trough, *WHT* Westholstein Trough. Elements of the gravity field: *GL* Glueckstadt Low; *HAH* Hamburg High; *HAL* Hamburg Low; *HH* Heide High; *HL* Helgoland Low; *ML* Moelln Low; *NKH* Norderstedt-Kiel High; *RFH* Ringkoebing-Fyn High; *SH* Sylt High.

Magnetic data

The map in Fig. 4b shows the aeromagnetic potential fields at a height of 700 m above the surface within the Glueckstadt Graben and adjacent areas with contour intervals of 10 nT. The magnetic field of the study area is characterised by a series of pronounced magnetic lows and highs (Fig. 4b). Several distinctive areas can be defined in the magnetic field of the Glueckstadt Graben. The eastern part is characterised by the presence of an almost NE–SW trending magnetic high. This zone of positive values has an elongated maximum (160 nT) within the northern part and a circular maximum (120 nT) near Hamburg. Towards the west, the study area is characterised by a chain of two positive and two negative magnetic anomalies. The two northern anomalies have higher magnitudes (110 and -80 nT) than the two southern ones (80 and -60 nT). These magnetic anomalies are individually characterised by NW–SE trends. On the other hand, the entire chain has almost a NE–SW trend coinciding with the trend of the elongated

positive anomaly in the east. The broad magnetic low (–60 nT) is clearly seen within the southwestern part of the Glueckstadt Graben.

3D gravity backstripping

A 3D gravity backstripping has been performed within the area covered by the 3D structural model of the Glueckstadt Graben and adjacent areas published by Maystrenko et al. (2005a, 2006). This basin-scale structural model provides a sufficient database for 3D gravity analysis. The latter has been carried out in order to estimate the gravity signals from different layers in the basin itself and crystalline crust/lithosphere below the Glueckstadt Graben. The 3D model has been constructed by use of structural data from the digital version of the Geotectonic Atlas of NW Germany (Baldschuhn et al. 1996, 2001), supplemented by use of well data and interpreted depth converted seismic sections (Maystrenko et al. 2005a, b, 2006). The model has a horizontal resolution of 2 km and originally contains the following seven layers: (1) the salt-rich Rotliegend plus the Zechstein, (2) the Triassic, (3) Jurassic, (4) Lower Cretaceous, (5) Upper Cretaceous, (6) Palaeogene and (7) Quaternary-Neogene.

Data and methods

During data preparation for the gravity modelling, the Palaeogene and the Quaternary-Neogene as well as the Lower and Upper Cretaceous have been merged into single layers (Fig. 5; Table 1). These four layers can be reduced to two because the lithology of these layers shows a gradual transition from carbonate-rich sediments to clastics in case of Cenozoic and vice versa in case of Cretaceous. Therefore, two layers with prevalence of clastics within the Cenozoic and prevalence of carbonates within the Cretaceous were introduced instead of four layers in order to reduce the time of calculations during 3D gravity analysis. On the other hand, an extremely thick layer of Triassic (up to 9,000 m) has been divided into two layers (Fig. 5; Table 1), the uppermost Middle-Upper Triassic (Keuper) and the Lower-Middle Triassic (Buntsandstein plus Muschelkalk), reflecting the presence of thick salt-rich layers within the Keuper deposits in order to make gravity calculations more accurate.

Density values have been assigned to the layers of the structural model (Table 1) based on density measurements of rock samples from industrial boreholes. These densities are in agreement with previously published data for the entire North German Basin (Inselmann 1985; Hermes

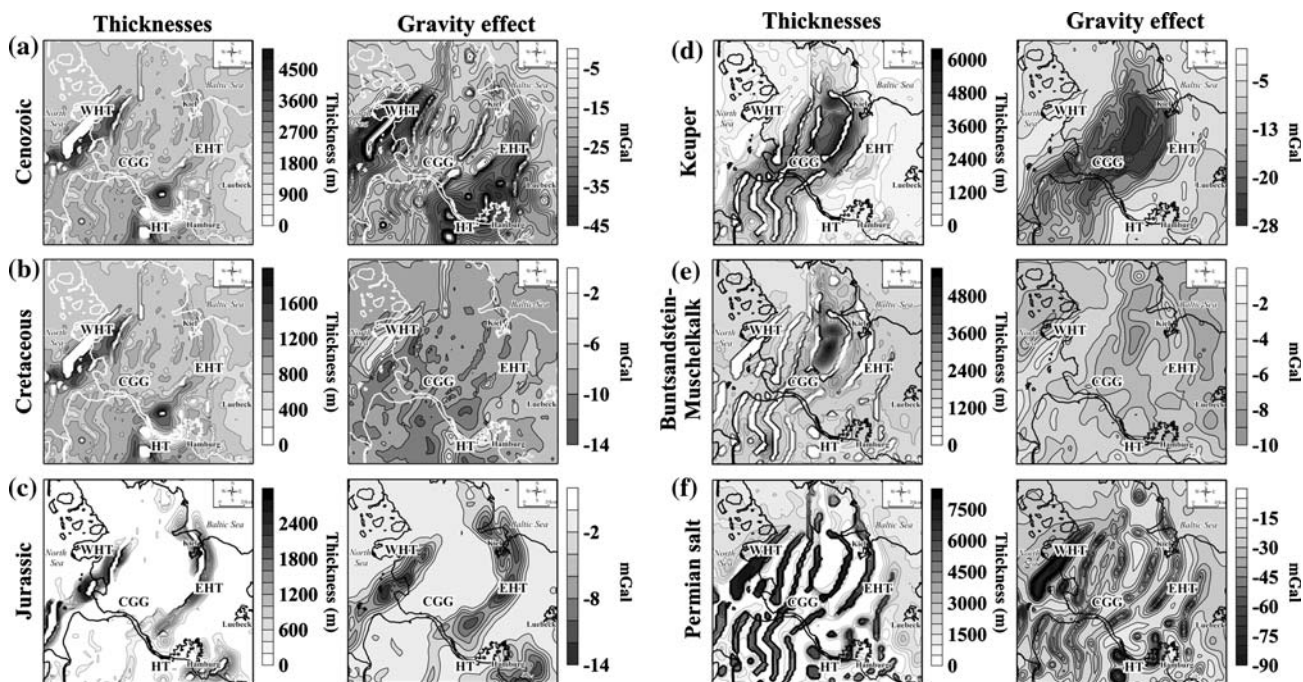


Fig. 5 Present-day thickness maps (left column) and gravity effects (right column) of the stratigraphic units of the 3D structural model: **a** Cenozoic layer with density $\rho = 2,000 \text{ kg/m}^3$ and exponential coefficient $k = 0.57$; **b** cretaceous sediments ($\rho = 2,320 \text{ kg/m}^3$, $k = 0.68$); **c** layer of Jurassic sediments ($\rho = 2,330 \text{ kg/m}^3$,

$k = 0.33$); **d** Keuper sediments ($\rho = 2,360 \text{ kg/m}^3$, $k = 0.47$); **e** Muschelkalk and Buntsandstein, $\rho = 2,560 \text{ kg/m}^3$, $k = 0.47$); **f** Permian (Zechstein and Rotliegend) with constant density $2,300 \text{ kg/m}^3$. CCG Central Glueckstadt Graben, EHT Eastholstein Trough, HT Hamburg Trough, WHT Westholstein Trough

Table 1 Density values of the stratigraphic units and 3D model layers of the Gluekstadt Graben

Layer	Period	Time unit	Lithology	Density, kg/m ³			Compaction
				From	To	Average for layer	
1	Cenozoic	Neogene	Clastics: clays and sandstones	2,010	2,110	2,000	0.57
		Paleogene	Clays, clay- and calcareous marls	1,990	2,250		
2	Mesozoic	Upper Cretaceous	Chalky limestones	2,320	2,490	2,320	0.68
		Lower Cretaceous	Claystones and marls	2,060	2,350		
3		Jurassic	Claystones and sandstones	2,260	2,400	2,330	0.33
4		Keuper	Claystones, clay marls, alteration of claystones and evaporites	2,250	2,490	2,360	0.47
5		Muschelkalk	Marlstones, limestones and layers of claystones and evaporites	2,550	2,740	2,560	0.47
		Bundsandstein	Claystones, clay marls and layers of evaporites	2,560	2,600		
6	Paleozoic	Zechstein	Evaporites (salt and anhydrite) and carbonates (mainly dolomite and limestone)	2,200	2,350	2,300	
		Rotliegend	Alteration of shales and evaporates (salt and anhydrite). Shales, sandstone and conglomerates.				

1986; Brink et al. 1994). The uppermost layer 1 (Cenozoic sediments) has the lightest average density (2,000 kg/m³) reflecting a clastic lithology. The prevalence of carbonates in the layer 2 (Cretaceous) results in an increased density up to 2,320 kg/m³. Approximately the same average density is typical for Jurassic claystones and sandstones (layer 3). The density of uppermost Middle-Upper Triassic sediments (Keuper, layer 4) depends strongly on the contribution of salt, which decreases the average density to 2,360 kg/m³. On the other hand, the density of the Middle and Lower Triassic sediments has a value of 2,560 kg/m³. The Permian salt has been calculated with a constant average density 2,300 kg/m³, representing some addition of carbonates and shales to the salt. Despite of density values, the data from industrial boreholes (Table 1) include information on the compaction state, which permits us to calculate the gravity effect of sediments by density-depth exponential function.

The three-dimensional gravity analysis utilises a “backstripping” technique, whereby the calculated effects of model layers, whose structure and properties are constrained by independent data, are successively removed from the observed gravity field. Previous investigations (Zhou and Thybo 1996; Yegorova et al. 1999, 2004, 2007) have demonstrated that backstripping is a suitable method in regions where lithosphere is hidden under thicker sediments. Calculated residual anomalies (observed anomalies minus the effect of the backstripped layers) can be related to density heterogeneities in the underlying layers (although “errors” in parameterising the backstripped layers cannot be excluded).

For calculating the gravity effect we use a software for solving the 3D direct gravity problem from layered medium with complex density distribution on both horizontal

and vertical directions (Starostenko and Manukyan 1987; Starostenko et al. 1997a, b; Starostenko and Legostaeva 1998a, b). An elementary body, used for gravity calculations, is represented by a vertical prism with arbitrary truncated upper and lower bases, where density varies with depth on linear or exponential functions. In this case the solution of direct gravity problem is reduced to the determination of double integral using cubature approach (Starostenko and Manukyan 1987). It is rather suitable to use this type of elementary body for describing the horizontally layered media, which are approximated by a set of elementary prisms, whose inclined surfaces (upper and lower) create in total the tilted contact surfaces of any complexity. For this study, we used elementary bodies with the dimensions of 2 × 2 km.

This program serves a kernel of an automated system developed by Starostenko et al. (1997b). The procedure involves the following steps: calculating the 3D gravity effect of the model defined by the upper and lower layer boundaries and layer densities (or density distributions); obtaining the summary and residual gravity field, and visualization of the model and modelling results.

For the 3D gravity analysis, we use 2,700 kg/m³ as a reference density of basement rocks. Anomalous densities for the model layers, calculated with regard to this reference density, vary in the range from –700 kg/m³ (Cenozoic sediments) to –140 kg/m³ (Middle and Lower Triassic rocks). Side effect elimination has been taken into account within a stripe of 25 km framing the model.

Gravity effect of sediments

Figure 5 shows that the thickness distribution of the sediments controls the intensity of the calculated gravity effect.

Where sediments are thick, the gravity effect is strong. Where sediments are relatively thin, low gravity effects are observed. In addition, the modelling method allows calculating density variation with depth by taking compaction into account.

The calculated gravity effect of the Cenozoic ($2,000 \text{ kg/m}^3$; $k = 0.57$) reaches maximum values (-40 mGal) in the Westholstein, Eastholstein and Hamburg Troughs, where the thickness of sediments is up to $5,000 \text{ m}$ (Fig. 5a). In contrast, the effect is much less intense in the central part of the Glueckstadt Graben and at the basin flanks. The area of the Central Glueckstadt Graben is characterised by narrow bands of very low gravity. There, the effect of the Cenozoic varies from -15 mGal to almost 0 above the crests of salt structures. Within the basin flanks, a similar pattern is observed towards the salt pillows. The reduction of the Cenozoic gravity effect above the crests of salt structures is in agreement with the thickness map where strong thinning of sediments occurs at the same places.

A slightly variable gravity effect of the Cretaceous ($2,320 \text{ kg/m}^3$; $k = 0.68$) is expressed in small variations (between -5 and -10 mGal) across the entire study area (Fig. 5b). However, an increased effect up to -14 mGal correlates with the thickened Cretaceous within the Westholstein and Hamburg Troughs. Within the central part and at the basin flanks, the thickness of the Cretaceous was less disturbed by salt movements, and therefore the gravity effect is more smoothed compared with the marginal troughs (Fig. 5b).

The Jurassic ($2,330 \text{ kg/m}^3$; $k = 0.33$) has strong gravity impact within the marginal troughs associated with thickened (up to $2,500 \text{ m}$) deposits, which remained after the regional Late Jurassic–Early Cretaceous erosion (Fig. 5c). The effect of the Jurassic sequence increases from less than -4 mGal to more than -12 mGal within the Westholstein, Eastholstein and the Hamburg Trough. On the other hand, the gravity effect ranges from 0 to -2 mGal over the central part of the Glueckstadt Graben and the basin shoulders.

Uppermost Middle–Upper Triassic (Keuper) strata ($2,330 \text{ kg/m}^3$; $k = 0.33$) provide the strongest impact in the central part of the basin due to a strong thickening of the sediments (up to $6,000 \text{ m}$, Fig. 5d). The study area is distinguished by a broad elongated, SW–NE directed anomaly within the Central Glueckstadt Graben, where the gravity effect reaches -27 mGal . Within the basin shoulders, where Keuper sediments have less thickness, the effect of Keuper varies only from -5 to -10 mGal .

The effect of the Lower–Middle Triassic (Buntsandstein plus Muschelkalk) layer was calculated with an average density of $2,560 \text{ kg/m}^3$ and a compaction coefficient of 0.47 . The intensity of the gravity effect is declining by moving away from the axial part towards the neighbouring salt structures (Fig. 5e), where the Buntsandstein and

Muschelkalk are absent or partially eroded as a result of the salt movements.

The thickness of the Permian salt and its gravity effect are shown in Fig. 5f. The Permian salt is represented by a single layer in the model. However, the Permian salt consists of two layers: salt-rich Rotliegend and Zechstein. These layers have been merged into one layer because it was difficult to separate them within the salt structures where the layers are mixed. The Zechstein consists mainly of salt with some carbonates, while salt-rich Rotliegend contains a remarkable amount of clastic material, which is represented mainly by shale. It is obvious that the clastics have higher density than pure salt. Therefore, the density of salt can vary to a certain extent within the salt structures depending on the amount of accompanying shale. As a starting point, we used a constant density ($2,300 \text{ kg/m}^3$) for the salt structures in 3D gravity backstripping modelling. This has been done due to some uncertainties related to the real shape and composition of salt structures. These salt-rich Permian rocks cause strong elongated anomalies over salt walls (up to -80 mGal) and almost circular anomalies (between -40 and -60 mGal) over salt diapirs and pillows (Fig. 5f). The gravity effect of salt verges towards -10 mGal within the areas where salt was almost withdrawn from the source layer.

Figure 6 shows the total gravity effect of the sediments. The most intense gravity anomalies are visible within the Westholstein Trough (-100 mGal) and in the Eastholstein Trough (-85 mGal). Over the axial part of the Glueckstadt Graben, the gravity effect is in the range 70 – 80 mGal . The total effect is gradually decreasing towards the basin flanks according to observed thinning of sediments in the same direction.

Residual gravity fields

The residual gravity field in the Fig. 7a was calculated by subtraction of the gravity effect of Meso–Cenozoic sediments and Permian salt (Fig. 6) from the observed field (Fig. 4a). This residual field reflects density heterogeneities below the basin (Permian base) within the crust and the upper mantle.

After removing the influence of the sedimentary fill, the Glueckstadt Graben appears as gravity high with two elongated maxima along the marginal troughs (Fig. 7a). Over the Westholstein Trough a pronounced positive anomaly evolves in comparison to the observed field (Fig. 7a). Similar to the observed field (see Heide High in Fig. 4a), this anomaly also dominates the sediment-free gravity field, reaching 100 mGal . Subtracting the effect of the sediments allows tracing the Heide gravity high further to the southwest over the Westholstein Trough more confidently. This is also true for the positive anomaly within

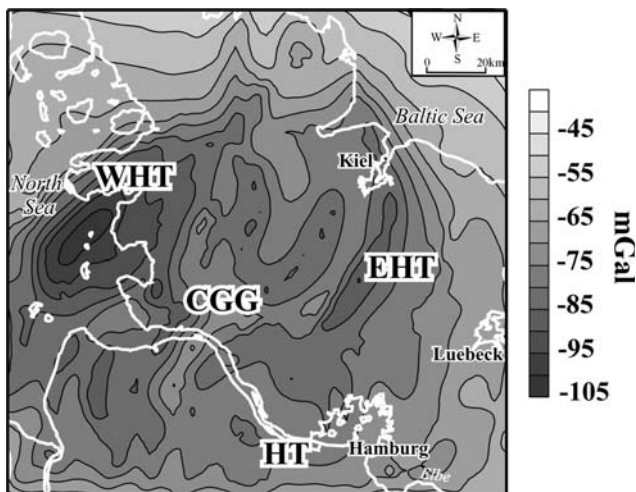


Fig. 6 Total gravity effect of sedimentary layers in the Glueckstadt Graben

the Eastholstein Trough, which is more pronounced now as compared to the observed field (cf. Figs. 4a, 7a). Two original anomalies over the marginal troughs joined within the northeastern part of the basin centre, reaching amplitude of 70 mGal. The intensity of the central part of this anomaly is decreasing towards the southeastern part of the basin centre where it gradually transforms into a relative gravity low (50 mGal). This relative gravity low corresponds to a broad GL in the observed field (cf. Figs. 4a, 7a), indicating that this gravity low cannot be explained by the gravity effect of Meso-Cenozoic sediments and Permian salt only. This suggests the presence of crustal density anomalies, which can be related to the older sediments and/or low-density crystalline crust within this part of the basin. The northwestern and southeastern basin flanks are represented by the residual gravity field with low values, which vary between 40 and 50 mGal.

In general, the wavelength of the gravity signal depends on the depth of the source body that produces it. Mostly, long wavelength signals correspond to deep sources. In order to distinguish the gravity anomalies from different depth levels, an attempt was made to separate the short wavelength signal of the residual gravity field due to sub-surface and upper-crust mass distribution.

After filtering for the long wavelength component using a filter window of 40 km, the Glueckstadt Graben is characterised by a broad positive gravity anomaly over the northeastern part of the basin centre, the Westholstein and Eastholstein Troughs (Fig. 7b). The intensity of the anomaly is highest within the northeastern part of the Westholstein Trough (90 mGal), where the Heide High is located in the observed field (cf. Figs. 4a, 7b). This should

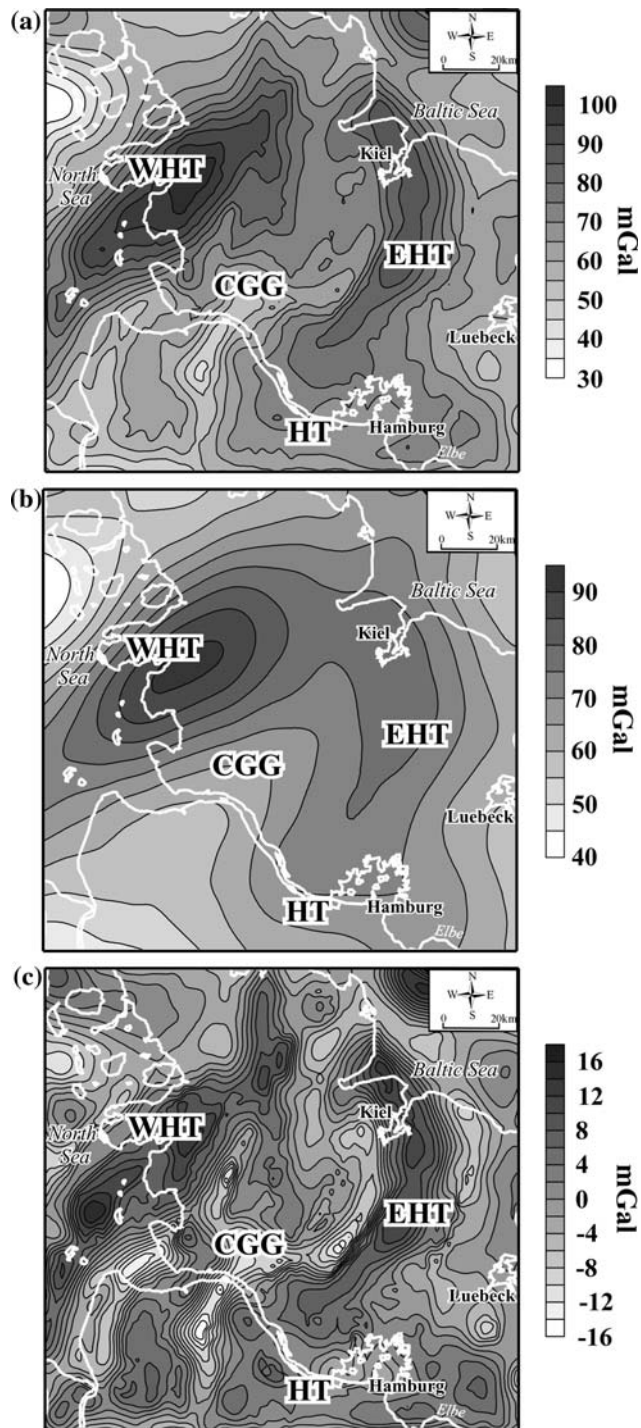


Fig. 7 a Residual gravity field (sediment-free anomalies) of the Glueckstadt Graben calculated by subtraction of the total gravity effect of the sediments (Fig. 6) from the observed gravity field (Fig. 4a); b long wavelength component of the residual gravity field (a), calculated using a filter window of 40 km; c short wavelength component responsible for small crustal heterogeneities, has been derived by subtracting the long wavelength component (b) from the residual gravity field (a)

indicate that the source of the HH is deeply rooted, confirming the results of previous gravity analysis within the study area in Dohr et al. (1989). At the basin scale, the long wavelength component of the residual field reveals that the Glueckstadt Graben is underlain by a high-density lower crust and/or upper mantle or a Moho uplift.

Removal of the long wavelength component (Fig. 7b) from the residual gravity field (Fig. 7a) emphasises two stripes of positive anomalies within the Westholstein (up to 14 mGal) and Eastholstein (up to 10 mGal) Troughs (Fig. 7c). Two minor local positive anomalies appeared along the axis of the basin—one within the northeastern part and one (up to 6 mGal) in the central part of the GL (cf. Figs. 4a, 7c). With the exception of the mentioned gravity highs, the rest of the Central Glueckstadt Graben area is characterised by low values of the gravity field. The complex pattern of the short wavelength component of the residual field indicates either a heterogeneous crust beneath the Glueckstadt Graben or remains from a shallower strata not filtered out.

Seismic pattern within the Glueckstadt Graben

Prior to the 2D potential field modelling, the seismic pattern of the area under consideration has to be discussed along the crucial reflection seismic profile, which crosses the central and eastern parts of the Glueckstadt Graben (see Fig. 3a for location). This line provides a regional overview of the area under consideration. The thickness differences shown in the profile provide the separation between the Central Glueckstadt Graben and the Eastholstein-Mecklenburg block. Consequently, the cross-section

can be subdivided into two main structural zones, which represent the Central Glueckstadt Graben with the superimposed Jurassic and Cenozoic Eastholstein Trough and the Eastholstein-Mecklenburg block. The pre-Permian strata have only been reached by very few wells within the Glueckstadt Graben. Consequently, correlation of pre-Permian reflections is not consistent due to the absence of well data and due to the presence of huge salt structures (see Fig. 8). The base of the salt-rich Rotliegend is the oldest horizon, which has been regionally dated within the Glueckstadt Graben. This horizon is constrained by drilling and seismic images (Maystrenko et al. 2005b). The base of the salt-rich Rotliegend usually marks the deepest correlatable reflections beneath the high-amplitude reflections from the Zechstein base. The geologic identification of the Zechstein base is well established in the Glueckstadt Graben due to the presence of a strongly reflective package consisting of two or three phases.

Clear evidences for basement fault-controlled subsidence have been recognised at the SE boundary of the Eastholstein Trough. There, a steep westward-dipping normal fault is observed, separating the Eastholstein Trough from the SE flank of the basin (Eastholstein-Mecklenburg block). Differential movements along the fault suggest a relatively young reactivation of this fault in Late Cenozoic times. It is important to note that the base of the salt-rich Rotliegend is almost horizontal close to the fault. On the other hand, the Zechstein base is well traceable and deformed within the hanging wall, indicating the dislocation of the Rotliegend salt. Thinning of both Zechstein and salt-rich Rotliegend strata further to the NW indicate a depletion of the salt-rich layers. The presence of salt structures makes the interpretation of the seismic reflec-

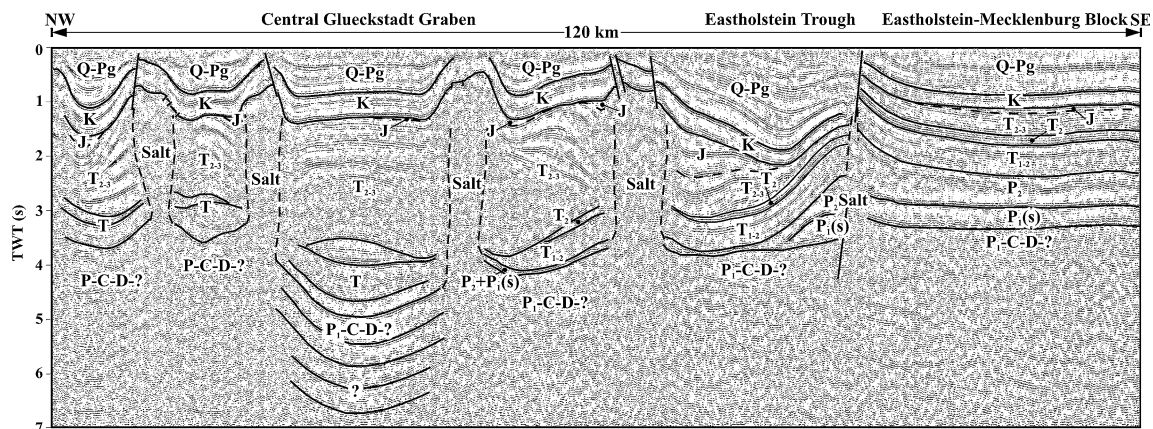


Fig. 8 Interpreted northwest-southeast seismic line across the Glueckstadt Graben. (modified after Maystrenko et al. 2005a) Stratigraphic key for this and other figures: P_1 -C-D Undivided Lower Rotliegend, Carboniferous and Devonian deposits; $P_1(s)$ salt-rich Rotliegend; P_2 Zechstein; $P_2 + P_1(s)$ upper part of the Lower Permian and Upper

Permian (undivided Zechstein and salt-rich Rotliegend); T_{1-2} Lower Triassic and lowermost part of Middle Triassic (Buntsandstein); T_2 Middle Triassic without uppermost and lowermost parts (Muschelkalk); $T_{2,3}$ uppermost part of Middle Triassic and Upper Triassic (Keuper); J Jurassic; K Cretaceous; Q -Pg Paleogene-Quaternary

tions rather difficult (Fig. 8). For that reason, the reflections beneath the base of the salt-rich Permian are not dated and the lower part of the Triassic is not subdivided within the deepest part of the Central Glueckstadt Graben. However, the presence of coherent reflections beneath the base of the salt-rich Permian suggests the presence of the Palaeozoic sediments within the Central Glueckstadt Graben. The exact age of these sediments is a matter of speculation. Certainly, they are not younger than Early Permian, and can be represented by Lower Permian, Carboniferous and Devonian successions.

The Lower Triassic (Buntsandstein) strata are characterised by variable thickness with some evidences of postsedimentation erosion near its deepest part (Fig. 8). The Muschelkalk shows a constant thickness at the basin shoulder and variable thickness towards the central part of the line. The uppermost Middle-Upper Triassic (Keuper) is characterised by strong variations in thickness and complex reflectivity images (Fig. 8). This sequence represents the infill of the Glueckstadt Graben and shows increasing thickness towards the basin centre. Towards the Central Glueckstadt Graben, the reflection patterns show evidence of strong syn-depositional thickening of the Keuper compare with the underlying strata. In contrast, the Keuper has a subparallel reflective package at the basin flank. The presence of baselapping strata of the thick Keuper sequence indicates rapid subsidence, accompanied by downbuilding of the salt structures.

Along the line, Jurassic sediments are only present around some salt structures, indicating the development of rim synclines along the edges of elongated salt walls. The presence of Jurassic on the SE flank of the basin indicates that the original infill probably covered a wider area before Late Jurassic-Early Cretaceous erosion. The Cretaceous sequence shows an almost constant thickness along the line with thinning from the Eastholstein Trough towards the SE flank. The deep Cenozoic Eastholstein Trough is characterised by thicken Cenozoic succession up to 2 s TWT on the eastern side of the line. Generally, the Cenozoic is characterised by thick sequences between the salt structures. Cenozoic rocks have been partially eroded from the crest of most of the salt structures (Fig. 8). The Cenozoic depressions between the salt walls indicate that the deposition of sediments occurred simultaneously with the growth of salt structures. In other words, the structure of the Cenozoic demonstrates the rim syncline character of deposition. By contrast, the Cenozoic strata have almost horizontal bedding within the axial part of the line and on the SE termination of the profile (Fig. 8).

In summary, it can be stated that this line shows that the post-Permian sedimentary succession of the Central Glueckstadt Graben and the Eastholstein Trough is deformed by salt movements. Thus, one of the main deformation

mechanisms in the area of the Glueckstadt Graben is salt tectonics. Various structural styles in the study area are related to movements of Permian salt. Details of the evolution are expressed in a variety of salt structures representing different stages of growth such as salt rollers, anticlines, pillows, stocks, and most pronounced elongated salt walls.

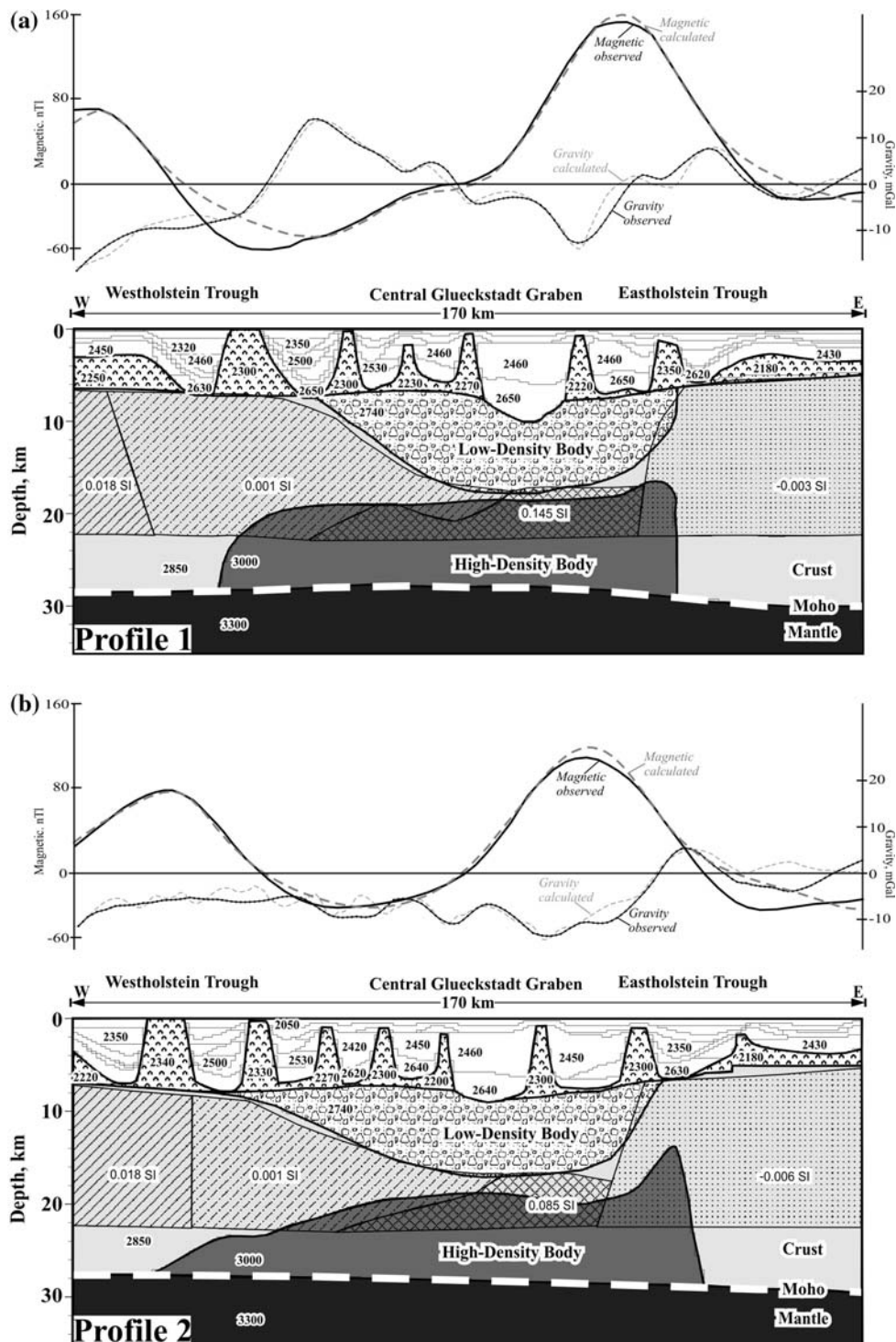
2D gravity and magnetic modelling

Here, the density model of the basin, supplemented by 2D magnetic modelling, has been analysed by use of two vertical slices from the 3D structural model. The position of the vertical slices is shown in Fig. 3a, also indicating their position relative to major tectonic units. In addition to the seismic line discussed above, profiles 1 and 2 provide cross-sectional views of the salt structure across basin strike (Fig. 3) and show the structural relations between the Central Glueckstadt Graben, the marginal troughs (the Westholstein and Eastholstein Troughs) and the basin flanks (Westschleswig and Eastholstein-Mecklenburg blocks) from the east to the west. These structural data (see profiles 1 and 2 in Fig. 9) indicate close relations between the thick sequences of the Triassic, Jurassic and Cenozoic across the Glueckstadt Graben. The thick Triassic succession of the central part overlying almost-depleted Permian evaporites thins towards the Westholstein and Eastholstein Troughs. Significant thinning broadly coincides with the axial parts of these marginal troughs. In contrast, the Jurassic deposits are cut by the Late Jurassic-Early Cretaceous erosion and are significantly thinning towards the Central Glueckstadt Graben. Prominent thickening of the Cenozoic occurs in limits of the Westholstein and Eastholstein Troughs along profiles 1 and 2 (Fig. 9).

Modelling results

Figure 9 shows 2D density models in the two cross-sections, derived from the 3D structural model (Maystrenko et al. 2006). The sedimentary cover of the Glueckstadt Graben is characterised by low density ($2,050 \text{ kg/m}^3$, Table 1) within the upper part of the Cenozoic, where sediments are relatively young, and therefore have low degree of compaction. The highest values of density ($2,650 \text{ kg/m}^3$) of the Meso-Cenozoic sediments are related to the Lower-Middle Triassic (the Buntsandstein and the Muschelkalk) within the central part of the basin and marginal troughs. The Buntsandstein and the Muschelkalk successions reach more than 10,000 m of depth in the basin centre. Consequently, the Lower-Middle Triassic deposits are overlain by thick sequence of younger sediments, which cause a high degree of compaction within the Central Glueckstadt

Fig. 9 Calculated and observed gravity and magnetic fields along two profiles for 2D density model across the Glueckstadt Graben, their location is shown in Fig. 3. Different density layers of the basin and lithospheric domains are shown by *shadings* and their densities—by numbers in kg/m^3 . Magnetic domains and their susceptibility are shown by *numbers* in SI units



Graben and the marginal troughs (the Wesholstein and the Eastholstein Troughs). Accordingly, the same stratigraphic interval (Buntsandstein-Muschelkalk) has smaller values of density of $2,450 \text{ kg}/\text{m}^3$ within the basin flanks where burial depth is less compared with the rest of the basin. The same is true for the other stratigraphic units along the profile,

where densities are increasing with burial depth. In contrast to the 3D gravity analysis with a constant salt density, the density of salt structures in Fig. 9 varies from $2,180$ to $2,350 \text{ kg}/\text{m}^3$ along the profiles, reflecting the portion of the upper Rotliegend clastics within the salt structures. In addition, the densities of Permian salt also depend on the

shape of salt structures because the shape of the salt structures was predefined with some approximation. This could cause some uncertainties concerning salt densities due to possible presence of overhang of Mesozoic sediments, which have not been considered during modelling. It was inferred from seismic and well data (Maystrenko et al. 2005b; Fig. 8) that Zechstein salt dominates within the basin flanks. The latter causes low densities ($2,180\text{--}2,250\text{ kg/m}^3$). On the other hand, higher densities (up to $2,330\text{ kg/m}^3$) are used within the Central Glueckstadt Graben (up to $2,300\text{ kg/m}^3$) and the marginal troughs (up to $2,350\text{ kg/m}^3$).

In our model, structural relationships and the depth of a low-density body is adopted from seismic profiles, which indicate a coherent reflectivity within the upper crust below the basin centre (e.g. Fig. 8). The interpretation is rather schematic, showing the presence of a low-density body from about 18 km of depth along the profile 1 (Fig. 9a) to 17 km of depth along the profile 2 (Fig. 9b). Deep reflections have been recognised with confidence within the central part of the basin, but towards the margins they lose their coherence due to poor seismic image. As a working hypothesis, the geometry of this body has been generalised westwards and eastwards from the basin centre as it is shown by the base of low-density body in Fig. 9. The 2D gravity modelling (Fig. 9) indicates that the Glueckstadt Graben is underlain by a high-density lower crust body with the density $3,000\text{ kg/m}^3$. Furthermore, the relative gravity minimum in the central part of the Glueckstadt Graben in Fig. 7c points towards a low-density body within the upper crust, indicating older sediments beneath the Triassic basin. The shape of the high-density body is in agreement with the results of 3D gravity backstripping, which indicate a high-density lower crust (Fig. 7b) beneath the entire Glueckstadt Graben with two local gravity maxima over the Westholstein and Eastholstein Troughs (Fig. 7c).

The results of 2D magnetic modelling indicate the presence of an area with high susceptibility ($0.085\text{--}0.145\text{ SI}$; see Fig. 9) mainly in the crystalline crust below the Central Glueckstadt Graben. During modelling, a constant Curie-isotherm has been taken at a depth of 22 km in accordance with previous magnetic studies within the North German Basin (Lindner et al. 2004; Scheibe et al. 2005). In addition, it was assumed that the sources of the observed magnetic anomalies (see Fig. 4b) are located within the crust rather than in the Meso-Cenozoic sedimentary strata. The latter is supported by the lithology of the sediments (Table 1). According to the results of magnetic modelling, the shape of the area with high magnetization is not symmetrical. This area is characterised by increased thickness towards the eastern part of the Central Glueckstadt Graben (Fig. 9).

Discussion

Modelling results indicate a high-density body within the lower crust of the Glueckstadt Graben (see Figs. 7b, 9). This high-density body is characterised by two well-defined crests at the east and the west, located beneath the Jurassic and Cenozoic depocentres (see Figs. 7c, 9). At the first glance, the shape of the high-density body can imply Jurassic or Cenozoic age of lower crust consolidation. Furthermore, the Cenozoic normal faulting within the marginal troughs (e.g., Fig. 8) can support that these crests were formed during the Cenozoic due to fault related intrusions of upper mantle material. As an additional hypothesis, the crests can also be related to the margins of the Triassic depocentre, and therefore may have Triassic age. On the other hand, the formation of such a huge high-density body is expected to be accompanied by strong volcanic activity on the surface or at least by formation of upper crustal intrusions. It is known from available borehole data that there is no evidence concerning magmatic activity during the Triassic, the Jurassic or the Cenozoic. The Lower Permian is the youngest interval where volcanic rocks have been drilled within the Glueckstadt Graben. Therefore, the Late Carboniferous–Early Permian regional rifting event can be related to the formation of the high-density body in the area under consideration. Here, we did not discuss in detail older tectonic events than Late Carboniferous (e.g., Variscan or Caledonian orogeny), which can also be considered in the context of this density pattern in the lower crust (Fig. 9). Based on all available data, we can suggest that the core of this body might have been formed during the Late Carboniferous—Early Permian regional rifting event (accompanied by contemporaneous magmatic activity). This rifting might have reworked older lower crust beneath the Glueckstadt Graben where high-velocity and density lower crust between Baltica and the Elbe Line is considered to be a remarkable regional structure associated with Baltica passive margin (Bayer et al. 2002). Further contributions to the formation of the high-density lower crust beneath the study area occurred probably during the Triassic, Jurassic and Cenozoic extensional events, leading to upwelling of the upper mantle melts into the lower crust. Certainly, this suggestion does not exclude older events, leading to differentiation of the lower crust in the region. Additionally, metamorphism of the lower crust might have resulted in the increase of a rock density and subsequently in the development of the identified high-density body (Brink 2005).

Another critical point of modelling is related to the geological interpretation of the low-density body beneath the Glueckstadt Graben. The infill of the low-density body can contain both Lower Permian and pre-Permian (Devonian or Carboniferous) rocks. However, the composition of

the low-density body is a matter of speculation based on the present-day state of our knowledge, and therefore cannot be defined correctly without additional investigations.

It is important to note that the high-density body beneath the central part of the basin can be replaced by a strong Moho uplift. But, in this case the Moho uplift would be accompanied by two local high-density bodies at the eastern and western margins. This will contradict all known observations of the lower crust beneath continental basins. Furthermore, deep seismic reflection experiments (DEKORP'96, Dobreflection-2000) within the North-East German Basin and the Donbas fold belt have shown that these continental basins are characterised by a flat Moho (DEKORP-BASIN Research Group 1999; Bayer et al. 1999; Maystrenko et al. 2003; DOBREFraction'99 Working Group 2003). This can be explained by flattening of the syn-rift uplifted Moho during the post-rift thermal subsidence according to McKenzie 1978. In addition, Yoon et al. (2005) have shown that the Moho is relatively flat with small uplift beneath the Glueckstadt Graben, and the lower crust is characterised by strong reflectivity. The latter pattern can be related to the high-density body, which is indicated in our density model of the study area (see Fig. 9). Therefore, the Moho topography used in our 2D modelling is in agreement with recent results of seismic data reprocessing within the Glueckstadt Graben (Yoon et al. 2005) and with other examples from the world (DEKORP-BASIN Research Group 1999; Bayer et al. 1999; Maystrenko et al. 2003).

Conclusions

The results obtained from gravity analyses can be summarized as follows:

Subtracting of the gravity effects of the Meso-Cenozoic sediments together with Permian salt reveals a positive residual anomaly (Fig. 7a) within the Glueckstadt Graben. This anomaly includes two local maxima over the Westholstein and Eastholstein Troughs. The residual field of the southeastern part of the basin centre is characterised by a relative gravity low which corresponds to a broad GL in the observed field (cf. Figs. 4a, 7a), indicating that this gravity low can not be explained by the effect of Meso-Cenozoic sediments and Permian salt only.

According to the results of the 3D gravity backstripping, the Heide gravity high is the most prominent positive anomaly of the Glueckstadt Graben (Fig. 4a). The source of this positive anomaly is deeply rooted as it was shown by filtering residual gravity field for the long wavelength component (Fig. 7b). Furthermore, this anomaly is also traceable in short wavelength component revealed after

removal of the long wavelength component from the residual gravity field. This supports former results of gravity modelling within the Glueckstadt Graben (Dohr et al. 1989), which indicate the presence of an intrusion within the crust beneath the Heide High.

The 2D gravity models point to the presence of a high-density body within the lower crust of the Glueckstadt Graben and indicate the formation of the basin before the Triassic, leaving the question about the age of final consolidation of the lower crust beneath the Glueckstadt Graben. The latter correlates with coherent reflections on the seismic data. In addition, the results of 2D magnetic modelling indicate that the central part of the high-density body is overlain by an area with high susceptibility (0.08–0.145 SI; see Fig. 9). Most probable, the formation of this high-density body in the lower crust, which has complex asymmetric configuration with two local bodies beneath the marginal (West- and Eastholstein) troughs, is a result of complex poly-phase tectonic history of the study area.

Finally, the results of gravity modelling indicate that Permian salt is not homogeneous. 3D gravity analysis and, especially, 2D gravity modelling (Fig. 9) have distinguished the differences in degree of salt saturation in salt-rich bodies, and hence contribution of Rotliegend salt associated with alteration with shale. There is a tendency, that the highest densities of salt bodies (2,300–2,350 kg/m³) occur in the huge salt walls within the central part and marginal troughs (Eastholstein, Westholstein and Hamburg), which have undergone the most complicated evolution with several pulses of salt movement during post-Permian times (Trusheim 1960; Sannemann 1968; Brink et al. 1992; Kockel 2002; Maystrenko et al. 2006). Relatively high-density salt structures of the central part and marginal troughs (Fig. 9) demonstrate a strong contribution of clastic material from mobilised salt-rich Rotliegend in addition to almost pure Zechstein salt within the Glueckstadt Graben (Maystrenko et al. 2005b). On the other hand, the densities of salt bodies vary between 2,180 and 2,250 kg/m³ at the basin shoulders (Fig. 9), implying the strong input of Zechstein salt into the salt structures. This is supported by seismic and well data which show that the salt-rich Rotliegend is almost undisturbed at the basin shoulders, and therefore salt structures contains mainly Zechstein salt (Baldschuhn et al. 1996, 2001; Maystrenko et al. 2005b).

Acknowledgments The authors gratefully acknowledge the financial support of the German Research Council in the framework of the Priority Programme 1135—DFG-SPP 1135 “Dynamics of sedimentary systems under varying stress conditions by example of the Central European Basin system”. We are grateful to the DGMK as representative of the German Oil and Gas Industry for supporting us with data and allowing us to present industrial data (DGMK project 577). Special thanks go to the E&P-Gesellschaften for data assistance.

We would also like to thank Heinz-Jürgen Brink and one anonymous reviewer for providing valuable and constructive reviews, which helped to improve the quality of the manuscript considerably.

References

- Abramovitz T, Thybo H (1999) Pre-zechstein structures around the MONNA LISA deep seismic lines in the southern Horn Graben area. *Bull Geol Soc Den* 45:99–116
- Bachmann GH, Grosse S (1989) Struktur und Entstehung des Norddeutschen Beckens—geologische und geophysikalische Interpretation einer verbesserten Bouguer-Schwerekarte. *Veröff Akad Geowiss* 2:23–47
- Bachmann GH, Hoffmann N (1997) Development of the Rotliegend basin in Northern Germany. *Geol Jb D* 103:9–31
- Baldschuhn R, Frisch U, Kockel F (eds) (1996) *Geotektonischer Atlas von NW-Deutschland 1:3000000*. 4pp, 65 maps, Bundesanstalt für geowissenschaften und Rohstoffe, Hannover
- Baldschuhn R, Binot F, Fleig S, Kockel F (2001) *Geotektonischer Atlas von Nordwest-Deutschland und dem deutschen Nordsee-Sektor*. Reihe A 153:3–95
- Bayer U, Scheck M, Rabbel W, Krawczyk CM, Götze H-J, Stiller M, Beilecke Th, Marotta A-M, Barrio-Alvers L, Kuder J (1999) An integrated study of the NE-German Basin. *Tectonophysics* 314:285–307
- Bayer U, Grad M, Pharaoh TC, Thybo H, Guterch A, Banka D, Lamarche J, Lassen A, Lewerenz B, Scheck M, Marotta A-M (2002) The southern margin of the East European Craton: new results from seismic sounding and potential fields between the North Sea and Poland. *Tectonophysics* 360:301–314
- Blundell D, Freeman R, Mueller St (1992) *A continent revealed: the European Geotraverse*. Cambridge University Press, Cambridge, pp 1–275
- Brink H-J (2005) The evolution of the North German Basin and the metamorphism of the lower crust. *Int J Earth Sci* 94:1103–1116
- Brink H-J, Franke D, Hoffmann N, Horst W, Oncken O (1990) Structure and evolution of the North German Basin. In: Freeman R, Giese P, Mueller St (Eds) *The European geotraverse integrative studies*. European Science Foundation, Strasbourg, pp 195–212
- Brink H-J, Dürshner H, Trappe H (1992) Some aspects of the late and post-Variscan development of the Northwestern German Basin. *Tectonophysics* 207:65–95
- Brink H-J, Bachem HC, Lühring HJ, Held B (1994) Erweiterte Präzechstein Bougueranomalie Norddeutschlands. *Geowiss* 12(3):74–79
- Dadlez R (2003) Mesozoic thickness pattern in the Mid-Polish Trough. *Geol Q* 47(3):223–240
- Dadlez R, Narkiewicz M, Stephenson RA, Visser MT, van Wees J-D (1995) Tectonic evolution of the Mid-Polish Trough: modelling implications and significance for central European geology. *Tectonophysics* 252:179–195
- DEKORP-BASIN'96 Research Group (1999) Deep crustal structure of the northeast German Basin: new DEKORP-Basin'96 deep-profiling results. *Geology* 27(1):55–58
- Dirkzwager JB, Stephenson RA, Legostaeva OV (2000) The pre-Permian residual gravity field for the Dutch onshore and adjacent offshore. *Glob Planet Change* 27:53–66
- DOBREFraction'99 Working Group; Grad M, Gryn D, Janik T, Keller R, Lang R, Lyngsie SB, Omelchenko V, Starostenko VI, Stephenson RA, Stovba SM, Thybo H, Tolkunov A (2003) "DOBREFraction'99", velocity model of the crust and upper mantle beneath the Donbas Foldbelt (East Ukraine). *Tectonophysics* 371:81–110
- Dohr G, Bachmann GH, Grosse S (1989) *Das Norddeutsche Becken*. Veröffentlichungen-Niedersächsische Akademie der Geowissenschaften 2:4–47
- EUGENO-S Working Group (1988) Crustal structure and tectonic evolution of the transition between the Baltic Shield and North German Caledonides (the EUGENO-S project). *Tectonophysics* 150:253–348
- Evans D, Graham C, Armour A, Bathurst P (2003) *The Millennium Atlas: Petroleum geology of the central and northern North Sea*. The Geological Society of London, London, pp 1–990
- Gast R (1988) Rifting im Rotliegenden Niedersachsens. *Die Geowissenschaften* 4:115–122
- Gregersen S, Voss P, TOR Working Group (2002) Summary of project TOR: delineation of a stepwise, sharp, deep lithosphere transition across Germany-Denmark-Sweden. *Tectonophysics* 260:63–70
- Hermes HJ (1986) Calculation of pre-Zechstein Bouguer anomaly in northwest Germany. *First Break* 4(1):13–32
- Inselmann R (1985) Dichte-Messungen in der Bundesrepublik Deutschland. *Erdöl-Erdgas*. 101.Jg., Heft 3:76–79
- Kockel F (2002) Rifting processes in NW-Germany and the German North Sea sector. *Geologie en Mijnbouw* 81:149–158
- Kockel F (2003) Problems of diapirism in northern Germany. *Geologos* 6:57–88
- Krolikowski C, Grobelny A (1991) Preliminary results of the geophysical interpretation (stripping method) in respect to the pre-Permian basement of southwestern Poland. *Kwartalnik Geologiczny* 35(4):449–476
- Krzywiec P (2006) Structural inversion of the Pomeranian and Kuiavian segments of the Mid-Polish Trough-lateral variations in timing and structural style. *Geol Q* 50:151–168
- Lindner H, Scheibe R, Seidel K, Hoffmann N (2004) Berechnung von Relief, Tiefenlage und Magnetisierung des magnetisch wirksamen Kristallins für das Norddeutsche Becken. *Z. angew Geol* 50(1):65–73
- Lockhorst A (1998) *NW European Gas Atlas-Composition and Isotope Ratios of natural Gases*. GIS application on CD-ROM by the British Geological Survey, Bundesanstalt für Geowissenschaften und Rohstoffe, Danmarks og Gronlands Geologiske, Undersogelse, Netherlands Instituut voor Toegepaste geowissenschaften, Panstwowy Instytut Geologiczny, European Union
- Lyngsie SB, Thybo H, Lassen TM (2006) Regional geological and tectonic structures of the North Sea area from potential field modelling. *Tectonophysics* 413:147–170
- Maystrenko Y, Stovba S, Stephenson R, Bayer U, Menuoli E, Gajewski D, Huebsher C, Rabbel W, Sainot A, Starostenko V, Thybo H, Tolkunov A (2003) Crustal-scale pop-up structure in cratonic lithosphere: DOBRE deep seismic reflection study of the Donbas fold belt, Ukraine. *Geology* 31(8):733–736
- Maystrenko Y, Bayer U, Scheck-Wenderoth M (2005a) The Glueckstadt Graben, a sedimentary record between the North Sea and Baltic Sea in north Central Europe. *Tectonophysics* 397:113–126
- Maystrenko Y, Bayer U, Scheck-Wenderoth M (2005b) Structure and evolution of the Glueckstadt Graben due to salt movements. *Int J Earth Sci* 94:799–814
- Maystrenko Y, Bayer U, Scheck-Wenderoth M (2006) 3D reconstruction of salt movements within the deepest post-Permian structure of the Central European Basin System—the Glueckstadt Graben. *Neth J Geosci/Geologie en Mijnbou* 85(3):183–198
- Mazur S, Scheck-Wenderoth M, Krzywiec P (2005) Different modes of the Late Cretaceous-Early Tertiary inversion in the North German and Polish basins. *Int J Earth Sci* 94:782–798
- McKenzie DP (1978) Some remarks on the development of sedimentary basins. *Earth Planet Sci Lett* 40:25–32
- Olesen O, Smethurst MA, Torsvik TH, Bidstrup T (2004) Sveconorwegian igneous complexes beneath the Norwegian-Danish Basin. *Tectonophysics* 387:105–130

- Otto V (2003) Inversion-related features along the southern margin of the North German Basin (Elbe fault system). *Tectonophysics* 373:107–123
- Pharaoh TC (1999) Palaeozoic terranes and their lithosphere boundaries within the Trans-European Suture Zone (TESZ): a review. *Tectonophysics* 314:17–41
- Plein E (1990) The Southern Permian Basin and its paleogeography. Sediments and environmental geochemistry—selected aspects and case histories. Springer, Berlin, pp 124–133
- Plomerova J, Babuska V, Kouba D (2002) Seismic anisotropy of the lithosphere around the Trans-European Suture Zone (TESZ) based on teleseismic body-wave data of the TOR experiment. *Tectonophysics* 360:89–114
- Sannemann D (1968) Salt-stock families in northwestern Germany. In: Braunstein J, O'Brien G (eds) Diapirism and diapirs. AAPG publication, pp 261–270
- Scheck M, Barrio-Alvers L, Bayer U, Götze H-J (1999) Density structure of the Northeast German Basin: 3D modeling along the DEKORP line BASIN96. *Phys Chem Earth, Part A* 24(3):221–230
- Scheck M, Bayer U, Otto V, Lamarche J, Banka D, Pharaoh T (2002) The Elbe fault system in North Central Europe—a basement controlled zone of crustal weakness. *Tectonophysics* 360:281–299
- Scheibe R, Seidel K, Vormbaum M, Hoffmann N (2005) Magnetic and gravity modelling of the crystalline basement in the North German Basin. *Z dt Ges Geowiss* 156(2):291–298
- Scheck-Wenderoth M, Lamarche J (2005) Crustal memory and basin evolution in the Central European Basin System—new insights from a 3D structural model. *Tectonophysics* 397:143–165
- Shomali ZH, Roberts RG, Pedersen LB, the TOR Working Group (2006) Lithospheric structure of the Tornquist Zone resolved by nonlinear P and S teleseismic tomography along the TOR array. *Tectonophysics* 416:133–149
- Starostenko VI, Legostaeva OV (1998a) Calculation of the gravity field from a heterogeneous, arbitrarily truncated vertical rectangular prism. *Izvestiya, Physics of the Solid Earth* 34(12):991–1003
- Starostenko VI, Legostaeva OV (1998b) Direct gravity problem for heterogeneous arbitrary truncated vertical rectangular prism. *Izvestia. Physics of the Solid Earth* 12:31–44
- Starostenko VI, Manukyan AG (1987) Gravimetric problems for spherical celestial bodies and their application to the study of the Nectaris Basin mascon on the Moon. *Boll Geofis Teor Appl* 29(115):201–219
- Starostenko VI, Legostaeva OV, Zavorot'ko AN, Egorova TP (1997a) 3-D modelling techniques in gravity of heterogeneous media. *Annales Geophysicae Supplement I* to 15:15
- Starostenko VI, Matsello VV, Aksak IN, Kulesh VA, Legostaeva OV, Yegorova TP (1997b) Automation of the computer input of images of geophysical maps and their digital modelling. *Geophys J (Kiev)* 17:1–19
- Thybo H (2001) Crustal structure along the EGT profile across the Tornquist Fan interpreted from seismic, gravity and magnetic data. *Tectonophysics* 334:155–190
- Trusheim F (1960) Mechanism of salt migration in North Germany. *Bull AAPG* 44:1519–1540
- Vejbaek OV, Britze P (1994) Top of the pre-Zechstein rocks. Sub- and supercrop map: Danmarks Geologiske Undersogelse (DGU) Miljøministeriet, Copenhagen, DGU map series no. 45, 1 sheet, scale 1:750000
- Wybraniec S, Zhou S, Thybo H, Forsberg R, Perhuc E, Lee MK, Demianov GD, Strakhov VN (1998) New map compiled of Europe's gravity field. *Eos, Trans Am Geophys Union* 79(37):437–442
- Yegorova TP, Stephenson RA, Kozlenko VG, Starostenko VI, Legostaeva OV (1999) 3-D gravity analysis of the Dnieper-Donets Basin and Donbas Foldbelt, Ukraine. *Tectonophysics* 313:41–58
- Yegorova TP, Stephenson RA, Kostyuchenko SL, Baranova EP, Starostenko VI, Popolitov KE (2004) Structure of the lithosphere below the southern margin of the East European Craton (Ukraine and Russia) from gravity and seismic data. *Tectonophysics* 381:81–100
- Yegorova TP, Bayer U, Thybo H, Maystrenko Y, Scheck-Wenderoth M, Lyngsie SB (2007) Gravity signals from the lithosphere in the Central European Basin System. *Tectonophysics*
- Yoon M, Baykulov M, Brink H-J, Gajewski D (2005) New insight into the crustal structure of northern Germany by reprocessing of reflection lines—Do we need a new evolution model for the Glückstadtgraben? *Terra Nostra* 05:127–130
- Zhou S, Thybo H (1996) Calculation of residual gravity anomalies in Northern Jutland, Denmark. *First Break* 14:129–134
- Zhou S, Thybo H (1997) Pre-Zechstein geology of the south-east North Sea, offshore Denmark—a geophysical perspective. *First Break* 15:387–395
- Ziegler PA (1990) Geological Atlas of Western and Central Europe. Shell International Petroleum Mij. B.V. (dist. by Geol. Soc. Publ. House, Bath), The Hague, Netherlands, pp 1–239